Applied Physics Letters ARTICLE scitation.org/journal/apl

A Landau–Devonshire analysis of strain effects on ferroelectric $Al_{1-x}Sc_xN$

Cite as: Appl. Phys. Lett. **121**, 042902 (2022); doi: 10.1063/5.0098979
Submitted: 13 May 2022 · Accepted: 7 July 2022 ·
Published Online: 25 July 2022

View Online Export Citation CrossMark

Keisuke Yazawa,[1,2,a)] Andriy Zakutayev,[1] and Geoff L. Brennecka[2,a)]

AFFILIATIONS

[1]Materials Science Center, National Renewable Energy Laboratory, Golden, Colorado 80401, USA
[2]Department of Metallurgical and Materials Engineering, Colorado School of Mines, Golden, Colorado 80401, USA

Note: This paper is part of the APL Special Collection on Piezoelectric Thin Films for MEMS.
[a)]**Authors to whom correspondence should be addressed:** Keisuke.Yazawa@nrel.gov and geoff.brennecka@mines.edu

ABSTRACT

We present a thermodynamic analysis of the recently discovered nitride ferroelectric materials using the classic Landau–Devonshire approach. Electrostrictive and dielectric stiffness coefficients of $Al_{1-x}Sc_xN$ with a wurtzite structure ($6\,mm$) are determined using a free energy density function assuming a hexagonal parent phase ($6/mmm$), with the first-order phase transition based on the dielectric stiffness relationships. The results of this analysis show that the strain sensitivity of the energy barrier is one order of magnitude larger than that of the spontaneous polarization in these wurtzite ferroelectrics, yet both are less sensitive to strain compared to classic perovskite ferroelectrics. These analysis results reported here explain experimentally reported sensitivity of the coercive field to elastic strain/stress in $Al_{1-x}Sc_xN$ films and would enable further thermodynamic analysis via phase field simulation and related methods.

Landau–Devonshire thermodynamic modeling has been widely acknowledged as a valuable tool for the phenomenological description of the physics of ferroelectrics.[1] The approach has been validated across a wide range of ferroelectric materials from the first ferroelectric discovered, Rochelle Salt, to recent HfO_2-based materials.[2–4] Extension to what is now referred to as the Landau–Ginsburg–Devonshire model enables rigorous investigation of polarization boundaries and reorientation, phase transformations, and domain formation/evolution.[5–10] Most recently, full ranges of the double well function, an important outcome of the Landau–Devonshire theory, have been experimentally observed, including the unstable "spinodal" region[11] associated with negative capacitance.[12,13] Thus, the phenomenological Landau–Devonshire theory continues to be a valuable tool for understanding and predicting properties and behaviors of ferroelectric materials.

Since the discovery of $Al_{1-x}Sc_xN$ ferroelectrics,[14] investigation of wurtzite ferroelectrics has been of great interest due to their large spontaneous polarization values and process compatibility with existing Si technology.[15–22] One challenge with these materials is the large coercive field. In this context, thermodynamic analysis is an attractive approach to predict and understand changes in properties under thermodynamic variables, such as strain, electric field, and temperature. However, most of the thermodynamic coefficients have not yet been determined for the wurtzite ferroelectrics. Most recently, Wang *et al.* described the thermodynamic double well function for $Al_{1-x}Sc_xN$ using density functional theory (DFT) calculation results for the second- and fourth-order dielectric stiffness.[23] Although that effort is an important start, higher order terms are critical for some materials,[24,25] and coupling terms that are non-negligible in many ferroelectric systems have not yet been addressed. Indeed, limited ferroelectric property tuning under elastic strain/stress has been reported in $Al_{1-x}Sc_xN$,[14,16,26] but consistent descriptions remain elusive.

The Landau–Devonshire free energy density (hereafter, "density" will be omitted for brevity) of a ferroelectric material with a centrosymmetric parent phase, whose variables are polarization P_i and total strain ε_{ij} can be expressed as[27]

$$f = a_{ij}P_iP_j + a_{ijkl}P_iP_jP_kP_l + a_{ijklmn}P_iP_jP_kP_lP_mP_n + \frac{1}{2}c_{ijkl}\varepsilon_{ij}\varepsilon_{kl} - q_{ijkl}\varepsilon_{ij}P_kP_l, \quad (1)$$

where a_{ij}, a_{ijkl}, and a_{ijklmn} are the dielectric stiffness coefficients at constant strain, c_{ijkl} is the elastic stiffness at constant polarization, and q_{ijkl} is the electrostrictive coefficient. Note that the summation symbols for each term are omitted hereafter. In a stress-free state, the strain derivative of Eq. (1) is 0, namely,[7,28,29]

$$\frac{\partial f}{\partial \varepsilon_{ij}} = \sigma_{ij} = c_{ijkl}\varepsilon^0_{kl} - q_{ijkl}P_kP_l = 0\,, \tag{2}$$

and the strain satisfying the relationship is the spontaneous strain ε^0_{kl}, which is expressed as

$$\varepsilon^0_{kl} = s_{klmn}q_{mnop}P_oP_p = Q_{klop}P_oP_p, \tag{3}$$

where Q_{ijkl} is polarization–strain electrostrictive coefficient. Plugging Eq. (3) into Eq. (1) gives the free energy at the stress-free boundary condition f^{sf}, which is expressed as[7,28,29]

$$f^{sf} = a_{ij}P_iP_j + a^*_{ijkl}P_iP_jP_kP_l + a_{ijklmn}P_iP_jP_kP_lP_mP_n, \tag{4}$$

where a^*_{ijkl} is expressed as

$$a^*_{ijkl} = a_{ijkl} - \frac{1}{2}c_{mnop}Q_{mnij}Q_{opkl}. \tag{5}$$

From this representation of the free energy under stress-free conditions, the polarization reorientation in a relaxed crystal at any point during the switching event can be discussed.

In this work, we apply this classic approach to the recently discovered wurtzite nitride ferroelectric $Al_{1-x}Sc_xN$ and are able to explain the origins of experimentally observed changes in a coercive field with elastic strain while also predicting a first-order phase transition to the centrosymmetric prototype phase. We use Landau–Devonshire thermodynamic modeling to describe elastic strain effects on $Al_{1-x}Sc_xN$ ferroelectrics up to sixth-order polarization terms, including elastic and electromechanical coupling terms. The coefficients are determined based upon a range of DFT calculations and experimental results reporting electric, elastic, and piezoelectric properties. The electrostrictive coefficient and range of dielectric stiffness values are determined for $Al_{1-x}Sc_xN$. We find that—consistent with experimental reports—the coercive field is more sensitive than spontaneous polarization to elastic strain; we also determine that strain has a significantly smaller effect on all relevant properties of $Al_{1-x}Sc_xN$ than the classic perovskite $PbTiO_3$.

In wurtzite ferroelectrics, the 6/*mmm* hBN structure is assumed to be the reference parent structure.[14,30,31] Based on Eq. (4), the stress-free free energy f^{sf} can be explicitly written to account for coefficient degeneracy due to the crystal symmetry as

$$\begin{aligned} f^{sf} =& a_{11}\left(P_1^2 + P_2^2\right) + a_{33}P_3^2 + a^*_{1111}\left(P_1^4 + P_2^4\right) + a^*_{3333}P_3^4 \\ &+ a^*_{1122}P_1^2P_2^2 + a^*_{1133}\left(P_1^2P_3^2 + P_2^2P_3^2\right) + a_{111111}\left(P_1^6 + P_2^6\right) \\ &+ a_{333333}P_3^6 + a_{111122}\left(P_1^4P_2^2 + P_1^2P_2^4\right) + a_{111133}\left(P_1^4P_3^2\right. \\ &\left.+P_1^2P_3^4 + P_2^4P_3^2 + P_2^2P_3^4\right) + a_{112233}P_1^2P_2^2P_3^2. \end{aligned} \tag{6}$$

The spontaneous polarization in wurtzite is along the three directions. Under conditions with no in-plane polarization in the system ($P_1 = P_2 = 0$, $P_3 \neq 0$), namely, when there exists no in-plane electric field or shear strain, conditions compatible with a polar oriented fiber-textured film or single crystal, the stress-free free energy can be reduced to

$$f^{sf} = a_{33}P_3^2 + a^*_{3333}P_3^4 + a_{333333}P_3^6. \tag{7}$$

The local minimum of the free energy represents the spontaneous polarization P_s; thus,

$$\left.\frac{\partial f^{sf}}{\partial P_3}\right|_{P_3=P_s} = 0. \tag{8}$$

Also, the second derivative of the free energy, which corresponds to the inverse of the slope of the *P*–*E* curve, is the observed dielectric susceptibility along the wurtzite three directions, namely,

$$\left.\frac{\partial^2 f^{sf}}{\partial {P_3}^2}\right|_{P_3=P_s} = \frac{1}{\kappa_0\chi_{33}}, \tag{9}$$

where κ_0 and χ_{33} are the vacuum permittivity and material susceptibility, respectively. From differential Eqs. (8) and (9), the higher order dielectric stiffness coefficients a^*_{3333} and a_{333333} are expressed in terms of a_{33} as

$$a^*_{3333} = -\frac{8a_{33}\kappa_0\chi_{33} + 1}{8P_s^2\kappa_0\chi_{33}}, \tag{10}$$

$$a_{333333} = -\frac{4a_{33}\kappa_0\chi_{33} + 1}{12P_s^4\kappa_0\chi_{33}}. \tag{11}$$

Thus, by plugging equations (10) and (11) into (7), the polarization-free energy curve at the stress-free condition can be illustrated with only one unknown variable, a_{33}, and experimentally or computationally obtained dielectric constant and spontaneous polarization. Figure 1 shows the polarization-free energy for stress-free conditions across a wide range of various a_{33} values for Sc content $x = 0.2$ in $Al_{1-x}Sc_xN$. The range is limited to the negative value of a_{33} to focus on the ferroelectric region.[27] The spontaneous polarization and susceptibility values utilized here are from reported DFT calculation results,[32,33] though they are consistent with a number of experimental reports as well.[14,15,33] The second-order term starts significantly affecting the curve shape when $a_{33} < -1 \times 10^9$ J m C^{-2}, and the well depth gets deeper with a decrease in a_{33} value. This well depth relates to the intrinsic ferroelectric coercive field, which is difficult to determine unambiguously due to kinetic contributions (e.g., frequency dependence of coercive field[34]) and strong influence of defects and extrinsic contributions to polarization reversal.[35,36] However, the lower limit of the a_{33} value can be determined via the curve shape shown in Fig. 1. In one limiting case for $a_{33} = -1 \times 10^{10}$ J m C^{-2}, the free energy decreases again for $P > 1.6$ C m^{-2} due to the strong negative contribution of the second-order term to the free energy. This is irrational because infinite polarization becomes the most stable state, which physically corresponds to decomposition via cation/anion displacement. Thus, stability dictates that the limit of f^{sf} of P as P approaches ∞ needs to be positive, namely,

$$\lim_{P\to\infty} f^{sf} = \frac{\infty(4a_{33}\kappa_0\chi_{33} + 1)}{\mathrm{sgn}(\kappa_0\chi_{33})} > 0. \tag{12}$$

From this, the a_{33} range is simply determined as

$$a_{33} > -\frac{1}{4\kappa_0\chi_{33}}. \tag{13}$$

Also, the sign of a^*_{3333} determines the order of the ferroelectric–dielectric phase transition.[27] From the a_{33}–a^*_{3333} relationship written in Eq. (10), the phase transition order is determined as follows:

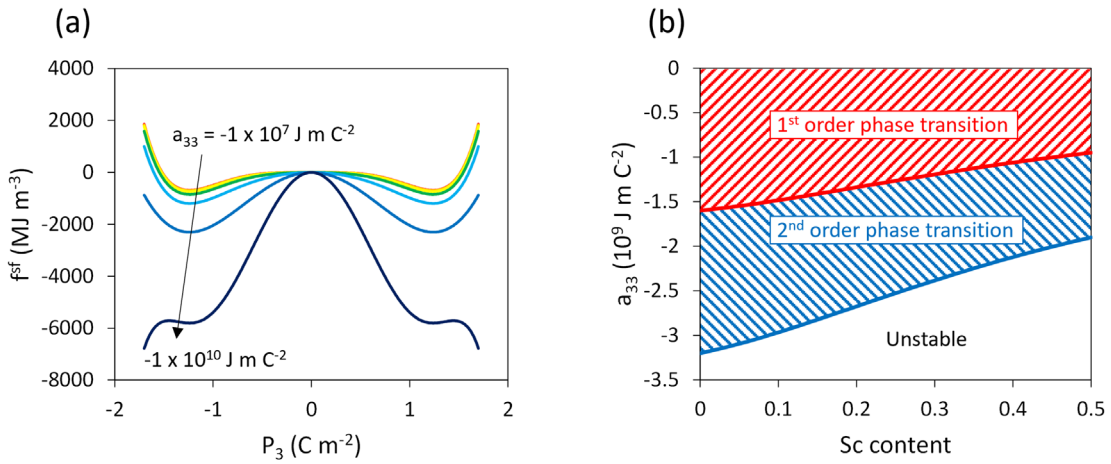

FIG. 1. Second-order dielectric stiffness a_{33} analysis. (a) Free energy curves with various a_{33} values for Sc content = 0.2. (b) First- and second-order phase transition ranges in a_{33} as a function of Sc content.

$$\begin{cases} a_{33} > -\dfrac{1}{8\kappa_0\chi_{33}}, & \text{first order phase transition,} \\ a_{33} < -\dfrac{1}{8\kappa_0\chi_{33}}, & \text{second order phase transition.} \end{cases} \tag{14}$$

Figure 1(b) illustrates the a_{33} lower limit and the first- and second-order transition ranges for the Sc range from $x = 0$–0.5. From a DFT calculated barrier height, the a_{33} value and phase transition order can be determined. Wang *et al.* reported 0.12 and 0.23 eV/f.u. for the barrier height of the double well function at $x = 0.2$ and 0 in a lattice relaxed transition that corresponds to the stress-free transition in this discussion.[23] Based on the DFT calculated barrier height, a_{33} at $x = 0.2$ is -0.32 GJ m C^{-2}, which is in the first-order phase transition range as shown in Fig. 1(b). It is noteworthy that the a_{33} value is comparable to that of classic perovskite ferroelectrics, such as -0.027 GJ m C^{-2} for $BaTiO_3$ and -0.17 GJ m C^{-2} for $PbTiO_3$.[29,37]

To understand the electro-mechanical coupling contribution to the spontaneous polarization, the electrostrictive coefficient needs to be determined. In the *6mm* wurtzite material system, the electrostrictive and piezoelectric coefficients are related as follows:[1,38]

$$d_{311} = d_{322} = 2Q_{1133}P_s\chi_{33}, \tag{15}$$

$$d_{333} = 2Q_{3333}P_s\chi_{33}. \tag{16}$$

In addition to the reported spontaneous polarization and susceptibility,[32,33] DFT simulation results for the piezoelectric coefficient[39,40] are used to calculate the electrostrictive coefficient. Figure 2 shows the electrostrictive coefficient as a function of Sc content. The absolute values of both Q_{3333} and $Q_{1133} = Q_{2233}$ increase with the increase in Sc content, similar to the Q and d increase in classic ferroelectric solid solutions, such as $PbZrO_3$–$PbTiO_3$.[33,39,41] It is noteworthy that the Q values at Sc content $x = 0.5$ (e.g., $Q_{3333} = 0.247$ m^4 C^{-2}) are significantly higher than those at the morphotropic phase boundary (MPB) of $Pb(Zr,Ti)O_3$ (e.g., $Q_{3333} = Q_{1111} = 0.097$ m^4 C^{-2}), which corresponds to the abrupt increase in piezoelectric coefficient in larger Sc content.[41,42] Polynomial fits from the composition–electrostrictive relationships are

$$Q_{3333} = 4.1068x^3 - 1.7514x^2 + 0.2846x + 0.0226, \tag{17}$$

$$Q_{1133} = -1.3904x^3 + 0.6022x^2 - 0.1021x - 0.0105, \tag{18}$$

where x is the Sc content ranging from 0 to 0.5. The values reported here are based upon the DFT calculated piezoelectric coefficient that Caro *et al.* reported.[39] For comparison, we also used the slightly different set of piezoelectric coefficients from Ambacher[40] and saw only a 6% difference in electrostrictive coefficient up to compositions of $x = 0.4$. This is less uncertainty than is commonly seen across different experimental reports. The dielectric stiffness and electrostrictive coefficient values for $x = 0$ to 0.5 are tabulated in Table I.

With the determined electrostrictive coefficient, elastic strain–spontaneous polarization coupling can be investigated. The explicit expression of Eq. (1) including the total strain as a variable can be simplified considering the crystal symmetry and polarization direction to

$$\begin{aligned} f = {} & a_{33}P_3^2 + a_{3333}P_3^4 + a_{333333}P_3^6 + \frac{1}{2}c_{1111}\left(\varepsilon_{11}^2 + \varepsilon_{22}^2\right) \\ & + \frac{1}{2}c_{3333}\varepsilon_{33}^2 + c_{1122}\varepsilon_{11}\varepsilon_{22} + c_{1133}\left(\varepsilon_{11}\varepsilon_{33} + \varepsilon_{22}\varepsilon_{33}\right) \\ & - q_{1133}(\varepsilon_{11} + \varepsilon_{22})P_3^2 - q_{3333}\varepsilon_{33}P_3^2. \end{aligned} \tag{19}$$

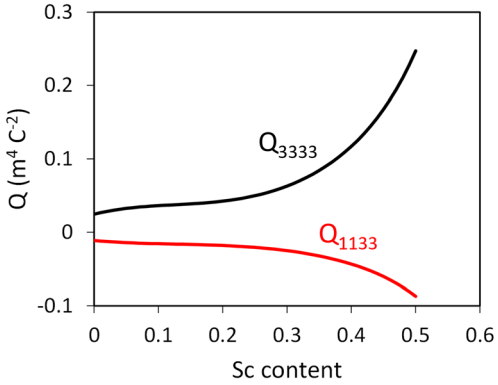

FIG. 2. Electrostrictive coefficient as a function of Sc content.

TABLE I. Range of dielectric stiffnesses and electrostrictive coefficients for x = 0 to 0.5.

		Sc content x in $Al_{1-x}Sc_xN$					
	Unit	0[a]	0.1	0.2[a]	0.3	0.4	0.5
a_{33}	GJ m C^{-2}	−1.84	>−2.97	−0.32	>−2.38	>−2.12	>−1.90
a^{a}_{3333}	GJ m^5 C^{-4}	0.33	<0.92	−0.66	<0.84	<0.89	<1.23
a_{333333}	GJ m^9 C^{-6}	0.12	>0	0.33	>0	>0	>0
a_{3333}	GJ m^5 C^{-4}	0.55	<1.13	−0.44	<1.19	<1.70	<3.28
Q_{3333}	m^4 C^{-2}	0.025	0.036	0.043	0.063	0.117	0.247
Q_{1133}	m^4 C^{-2}	−0.011	−0.016	−0.018	−0.025	−0.043	−0.087

[a]The dielectric stiffnesses are determined by energy barrier height of a DFT result at $x = 0$ and 0.2.[26]

Note that shear strain contributions to the free energy are omitted here due to the assumption that no in-plane polarization emerges. The fourth-order dielectric stiffness, a_{3333}, under fixed strain boundary conditions, can be back-engineered from Eq. (5) (with symmetry considerations) as

$$a_{3333} = a^*_{3333} + \frac{1}{2}\left(2c_{1111}Q^2_{1133} + 2c_{1122}Q^2_{1133} + 4c_{1133}Q_{1133}Q_{3333} + c_{3333}Q^2_{3333}\right). \quad (20)$$

Also, q_{1133} and q_{3333} can be represented in terms of Q_{1133} and Q_{3333}, and reported stiffness c_{ijkl} even though the other Q_{ijkl} components are unknown,[39] namely,

$$q_{1133} = c_{11mn}Q_{mn33}, \quad (21)$$

$$q_{3333} = c_{33mn}Q_{mn33}. \quad (22)$$

Although the entire free energy curve as a function of polarization at a fixed strain state represents a rare case (e.g., hydrostatically constrained crystal), the local minima give the spontaneous polarization at a static state with an arbitrary strain. Thus, spontaneous polarization $P^*_s(\varepsilon)$ satisfies the derivative equation

$$\left.\frac{\partial f}{\partial P_3}\right|_{P_3 = P^*_s} = 0, \quad (23)$$

namely, the spontaneous polarization as a function of total strain is expressed as

$$P^*_s(\varepsilon) = \sqrt{\frac{-a_{3333} + \sqrt{a^2_{3333} - 3a_{333333}(a_{33} - q_{1133}(\varepsilon_{11}+\varepsilon_{22}) - q_{3333}\varepsilon_{33})}}{3a_{333333}}}. \quad (24)$$

Note that the higher order dielectric stiffness coefficients can be written with only one coefficient a_{33} unknown for the entire composition range as shown in Eqs. (10), (11), and (20). From the spontaneous polarization, the free energy barrier for the double well is expressed as

$$f_b = f(0) - f(P^*_s). \quad (25)$$

Note that the free energy barrier f_b represents the polarization switching barrier at a fixed strain for the entire event. This value tends to be higher than that in actual stress-free switching due to the larger elastic energy contribution during switching. Nevertheless, the value should relate to the ferroelectric switching coercive field, and comparison across composition and strain states under identical conditions provides a trend.

The total strain ε_{ij} is a sum of an elastic strain $\varepsilon^{ela}{}_{ij}$ and spontaneous strain $\varepsilon^{0}{}_{ij}$ under isothermal conditions (where there is no thermal strain contribution), namely,

$$\varepsilon_{ij} = \varepsilon^{ela}_{ij} + \varepsilon^{0}_{ij}. \quad (26)$$

Considering the relationship $\varepsilon^{ela}{}_{ij}$ to $P^*_s(\varepsilon)$ is more useful for intuitive understanding of the strain–spontaneous polarization relationship because the measured strain is an elastic strain added to already spontaneously strained states. From Eqs. (3), (24), and (26), an elastic strain tensor component is expressed as

$$\varepsilon^{ela}_{ij} = \varepsilon_{ij} - Q_{ij33} \times \frac{-a_{3333} + \sqrt{a^2_{3333} - 3a_{333333}(a_{33} - q_{1133}(\varepsilon_{11}+\varepsilon_{22}) - q_{3333}\varepsilon_{33})}}{3a_{333333}}. \quad (27)$$

As expressed in Eqs. (24), (25), and (27), spontaneous polarization, free energy barrier, and elastic strain are uniquely determined at an arbitrary total strain state with an assumed a_{33} value. Recall the assumption that no shear strain components exist to preserve $P_1 = P_2 = 0$ in the model.

The existence of an elastic strain effect on spontaneous polarization is not surprising since strain–polarization coupling is common in ferroelectrics[6,43,44] and already reported in the wurtzite ferroelectrics.[14,16,26] However, our quantitative analysis provides important information about the magnitude of the effects of strain compared to other factors, such as chemistry. Figure 3(a) shows elastic strain–spontaneous polarization maps for $Al_{0.8}Sc_{0.2}N$ and $PbTiO_3$ for comparison. The coefficients of $PbTiO_3$ are from the literature[45,46] after converting compliance from constant electric field s^E to constant polarization s^D for direct comparison to our model.[47] The spontaneous polarization values are normalized with the spontaneous polarization in a stress-free state. The degree of spontaneous polarization change under an elastic strain is different; $Al_{0.8}Sc_{0.2}N$ undergoes −2.7 to +2.5% of change in spontaneous polarization under 1% elastic strain, whereas $PbTiO_3$ exhibits −10 to +7.5% of change in P_s under the same percentage strain. This means that the polarization of $Al_{0.8}Sc_{0.2}N$ is less susceptible to elastic strain compared to $PbTiO_3$.

Figure 3(b) shows the composition dependence of spontaneous polarization with envelopes representing maximum and minimum

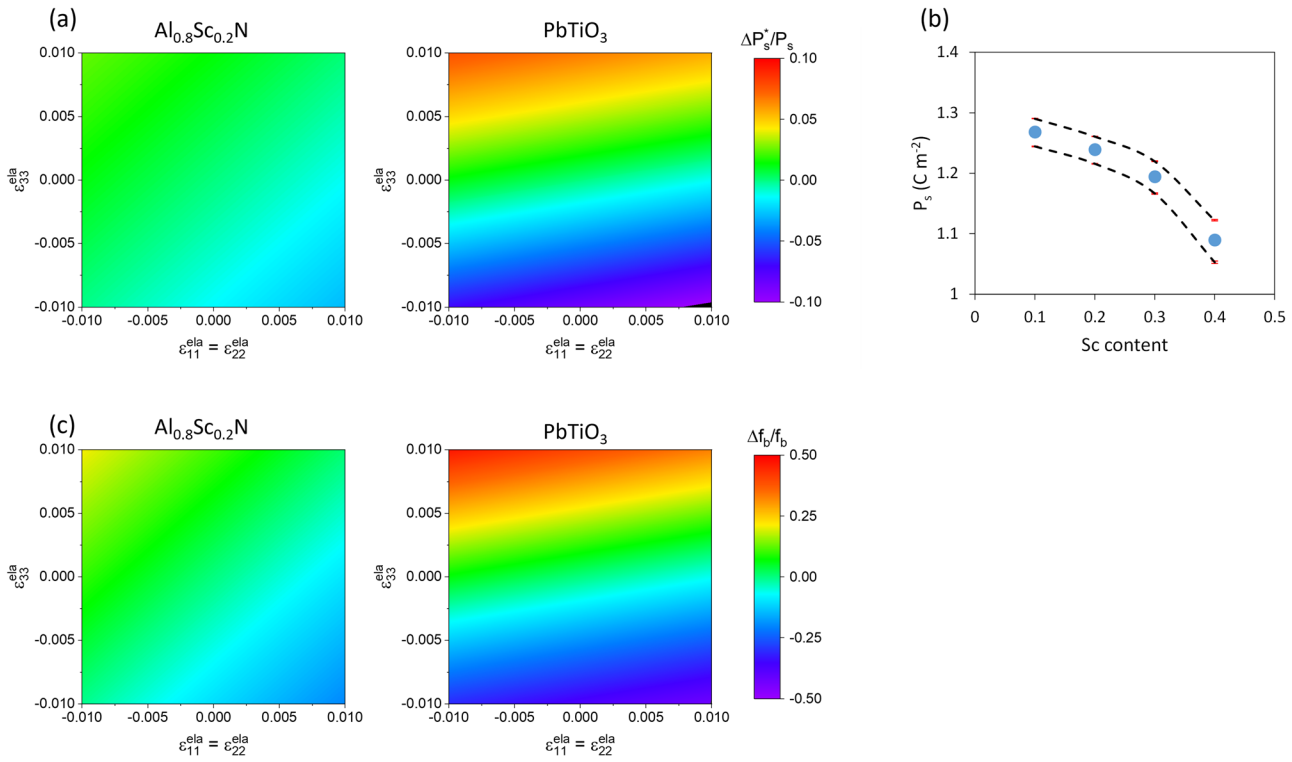

FIG. 3. Elastic strain effects on ferroelectric properties. (a) Normalized spontaneous polarization map for $Al_{0.8}Sc_{0.2}N$ and $PbTiO_3$ under ±1% of elastic strain. (b) Spontaneous polarization as a function of Sc content. Envelope (dashed lines) shows the maximum and minimum values under ±1% of uniaxial elastic strain $\varepsilon^{ela}{}_{33}$. (c) Normalized free energy barrier map for $Al_{0.8}Sc_{0.2}N$ and $PbTiO_3$ under ±1% of elastic strains.

polarization values under ±1% of $\varepsilon^{ela}{}_{33}$ and ∓0.3% of $\varepsilon^{ela}{}_{11} = \varepsilon^{ela}{}_{22}$. The error bars along with the envelopes show the possible range due to the range of the unknown a_{33} value in the composition range except $x = 0.2$ as shown in Table I. The error bars are quite small compared to the chemistry and strain effects as discussed in the supplementary material. The strain corresponds to uniaxial strain along the three directions with assumed Poisson's ratio equal to 0.3. The plotted dots are the stress-free spontaneous polarization from DFT calculations.[32] From Sc content $x = 0.1$ to 0.4, a 14% decrease in spontaneous polarization is seen, and this change is more than five times larger than the change attributed to ±1% of uniaxial elastic strain along the polar direction. Note that 1% of uniaxial elastic strain corresponds to 1.2–2.7 GPa, which is close to the fracture strength of AlN thin films[48] and more than the controllable range in residual stress with sputtering process variables.[49] Therefore, composition is more effective than lattice strain for controlling spontaneous polarization in $Al_{1-x}Sc_xN$. Lattice strain can tune spontaneous polarization up to a couple of percent, which is smaller than classic perovskite ferroelectrics $PbTiO_3$.

Figure 3(c) illustrates the elastic strain-free energy barrier f_b maps for $Al_{0.8}Sc_{0.2}N$ and $PbTiO_3$ for comparison. The f_b values are normalized with the free energy barrier under the condition that the total strain is only spontaneous strain at a stress-free state. Both materials show a larger barrier height with larger spontaneous strain. In a range of ±1% elastic strain, the elastic effect on f_b is −19 to +20% for $Al_{0.8}Sc_{0.2}N$, while that for $PbTiO_3$ is −42 to +45%. Again, $Al_{0.8}Sc_{0.2}N$ shows smaller effects of elastic stain than does $PbTiO_3$, but the percent change in barrier height under an elastic strain is one order of magnitude larger than the percent change in spontaneous polarization, so the difference between the strain sensitivity between $Al_{1-x}Sc_xN$ and $PbTiO_3$ is significantly less for the barrier to polarization reversal than to the spontaneous polarization value itself. The free energy barrier is investigated only at $x = 0.2$ since the unknown a_{33} value is critical for free energy barrier analysis as discussed in the supplementary material.

Indeed, a recent experimental report suggested that the ionicity of Sc–N bonding is the dominant factor that controls spontaneous polarization in this system.[50] The result showing decreased spontaneous polarization with the increase in Sc content even in an elastically strained film is consistent with Fig. 3(b). The coercive field, however, is commonly reported to be sensitive to elastic strain/stress,[14,16,26] consistent with the greater sensitivity of the free energy barrier to strain that we show here. A quantitative relationship between the coercive field and thermodynamic calculations requires knowledge of the switching mechanism(s) and the intermediate state or static domain boundary configuration (e.g., the intermediate strain state during polarization switching attributed to a change in spontaneous strain as well as the elastic interaction across domain walls). Moreover, the intermediate state might possess in-plane polarization components, i.e., P_1 and/or $P_2 \neq 0$, thereby requiring in-plane coupling and dielectric stiffness coefficients for further studies dealing with switching dynamics and domain evolution. Nevertheless, from the thermodynamic perspective, the technique presented in this study can be generalized to predict the

ferroelectric response with regard to thermodynamic variables, based on the wide applicability of the Landau–Devonshire approach on ferroelectrics.

Free energy analysis of $Al_{1-x}Sc_xN$ with an electromechanical coupling term using the Landau–Devonshire formalism has been carried out based on reported DFT calculation results. Dielectric stiffness coefficients are determined based on the free energy curve shape under stress-free conditions, keeping the double well function for $x = 0$–0.5. A first-order thermally driven phase transition between the polar ferroelectric phase *6 mm* and non-polar parent *6/mmm* phase is expected at $x = 0.2$ based on the dielectric stiffness coefficients. The electrostrictive coefficients for $x = 0$–0.5 are determined using reported piezoelectric coefficients, spontaneous polarization values, and dielectric susceptibility. The ambiguity due to the range of a_{33} value is shown to be unimportant for the elastic strain–spontaneous polarization curve, and the elastic strain effect on spontaneous polarization is small compared to $PbTiO_3$. The elastic strain effect on free energy barrier height is also small for $Al_{1-x}Sc_xN$ compared to $PbTiO_3$, but the relative difference is not as large. These results explain the experimentally reported coercive field tunability under elastic strain/stress as well as the relative stability of spontaneous polarization with strain. Determination of the sensitivity of various properties to external variables such at strain provides crucial guidance for how to optimize properties for potential future applications.

See the supplementary material for further analysis for the a_{33} sensitivity for the spontaneous polarization and free energy barrier.

This work was co-authored by Colorado School of Mines and the National Renewable Energy Laboratory, operated by the Alliance for Sustainable Energy, LLC, for the U.S. Department of Energy (DOE) under Contract No. DE-AC36-08GO28308. Funding was provided by the DARPA Tunable Ferroelectric Nitrides (TUFEN) program (No. DARPA-PA-19-04-03. K.Y.), the National Science Foundation (No. NSF DMR-1555015, G.L.B.), and the Office of Science (SC), Office of Basic Energy Sciences (BES) as part of the Early Career Award "Kinetic Synthesis of Metastable Nitrides" (A.Z.).

AUTHOR DECLARATIONS

Conflict of Interest

The authors have no conflicts to disclose.

Author Contributions

Keisuke Yazawa: Conceptualization (lead); Data curation (lead); Formal analysis (lead); Investigation (lead); Methodology (lead); Validation (lead); Visualization (lead); Writing – original draft (lead); Writing – review and editing (equal). **Andriy Zakutayev:** Funding acquisition (supporting); Supervision (equal); Writing – review and editing (equal). **Geoff Brennecka:** Funding acquisition (lead); Supervision (equal); Writing – original draft (supporting); Writing – review and editing (equal).

DATA AVAILABILITY

The data that support the findings of this study are available from the corresponding authors upon reasonable request. The views expressed in the article do not necessarily represent the views of the DOE or the U.S. Government.

REFERENCES

[1]A. F. Devonshire, London, Edinburgh, Dublin Philos. Mag. J. Sci. **40**, 1040 (1949).
[2]A. F. Devonshire, Adv. Phys. **3**, 85 (1954).
[3]M. J. Haun, E. Furman, H. A. McKinstry, and L. E. Cross, Ferroelectrics **99**, 27 (1989).
[4]P. D. Lomenzo, M. Materano, C. Richter, R. Alcala, T. Mikolajick, and U. Schroeder, Appl. Phys. Lett. **117**, 142904 (2020).
[5]A. J. Bell, J. Appl. Phys. **89**, 3907 (2001).
[6]N. A. Pertsev, A. G. Zembilgotov, and A. K. Tagantsev, Phys. Rev. Lett. **80**, 1988 (1998).
[7]S. Nambu and D. A. Sagala, Phys. Rev. B **50**, 5838 (1994).
[8]Y. L. Li, S. Choudhury, Z. K. Liu, and L. Q. Chen, Appl. Phys. Lett. **83**, 1608 (2003).
[9]J. Wang, S.-Q. Shi, L.-Q. Chen, Y. Li, and T.-Y. Zhang, Acta Mater. **52**, 749 (2004).
[10]E.-M. Anton, R. E. García, T. S. Key, J. E. Blendell, and K. J. Bowman, J. Appl. Phys. **105**, 024107 (2009).
[11]M. Hoffmann, F. P. G. Fengler, M. Herzig, T. Mittmann, B. Max, U. Schroeder, R. Negrea, L. Pintilie, S. Slesazeck, and T. Mikolajick, Nature **565**, 464 (2019).
[12]A. I. Khan, K. Chatterjee, B. Wang, S. Drapcho, L. You, C. Serrao, S. R. Bakaul, R. Ramesh, and S. Salahuddin, Nat. Mater. **14**, 182 (2015).
[13]M. Hoffmann, M. Pešić, K. Chatterjee, A. I. Khan, S. Salahuddin, S. Slesazeck, U. Schroeder, and T. Mikolajick, Adv. Funct. Mater. **26**, 8643 (2016).
[14]S. Fichtner, N. Wolff, F. Lofink, L. Kienle, and B. Wagner, J. Appl. Phys. **125**, 114103 (2019).
[15]S. Yasuoka, T. Shimizu, A. Tateyama, M. Uehara, H. Yamada, M. Akiyama, Y. Hiranaga, Y. Cho, and H. Funakubo, J. Appl. Phys. **128**, 114103 (2020).
[16]K. Yazawa, D. Drury, A. Zakutayev, and G. L. Brennecka, Appl. Phys. Lett. **118**, 162903 (2021).
[17]D. Drury, K. Yazawa, A. Mis, K. Talley, A. Zakutayev, and G. L. Brennecka, Phys. Status Solidi RRL **15**, 2100043 (2021).
[18]J. Hayden, M. D. Hossain, Y. Xiong, K. Ferri, W. Zhu, M. V. Imperatore, N. Giebink, S. Trolier-Mckinstry, I. Dabo, and J. P. Maria, Phys. Rev. Mater. **5**, 044412 (2021).
[19]K. Ferri, S. Bachu, W. Zhu, M. Imperatore, J. Hayden, N. Alem, N. Giebink, S. Trolier-McKinstry, and J.-P. Maria, J. Appl. Phys. **130**, 044101 (2021).
[20]W. Zhu, J. Hayden, F. He, J. I. Yang, P. Tipsawat, M. D. Hossain, J. P. Maria, and S. Trolier-McKinstry, Appl. Phys. Lett. **119**, 062901 (2021).
[21]D. Wang, P. Musavigharavi, J. Zheng, G. Esteves, X. Liu, M. M. A. Fiagbenu, E. A. Stach, D. Jariwala, and R. H. Olsson, Phys. Status Solidi RRL **15**, 2000575 (2021).
[22]J. X. Zheng, D. Wang, P. Musavigharavi, M. M. A. Fiagbenu, D. Jariwala, E. A. Stach, and R. H. Olsson, J. Appl. Phys. **130**, 144101 (2021).
[23]H. Wang, N. Adamski, S. Mu, and C. G. Van de Walle, J. Appl. Phys. **130**, 104101 (2021).
[24]A. J. Bell and L. E. Cross, Ferroelectrics **59**, 197 (1984).
[25]D. Vanderbilt and M. H. Cohen, Phys. Rev. B. **63**, 094108 (2001).
[26]S. Rassay, F. Hakim, C. Li, C. Forgey, N. Choudhary, and R. Tabrizian, Phys. Status Solidi RRL **15**, 2100087 (2021).
[27]G. Shirane and F. Jona, *Ferroelectric Crystals* (Macmillan, New York, 1962).
[28]W. Cao and L. E. Cross, Phys. Rev. B **47**, 4825 (1993).
[29]J. Hlinka and P. Márton, Phys. Rev. B **74**, 104104 (2006).
[30]C. E. Dreyer, A. Janotti, C. G. Van de Walle, and D. Vanderbilt, Phys. Rev. X **6**, 021038 (2016).
[31]H. Moriwake, R. Yokoi, A. Taguchi, T. Ogawa, C. A. J. Fisher, A. Kuwabara, Y. Sato, T. Shimizu, Y. Hamasaki, H. Takashima, and M. Itoh, APL Mater. **8**, 121102 (2020).
[32]K. Furuta, K. Hirata, S. A. Anggraini, M. Akiyama, M. Uehara, and H. Yamada, J. Appl. Phys. **130**, 024104 (2021).
[33]M. Akiyama, K. Umeda, A. Honda, and T. Nagase, Appl. Phys. Lett. **102**, 021915 (2013).

[34]J. F. Scott, Integr. Ferroelectr. **12**, 71 (1996).
[35]K. Kitamura, Y. Furukawa, K. Niwa, V. Gopalan, and T. E. Mitchell, Appl. Phys. Lett. **73**, 3073 (1998).
[36]S. Kim, V. Gopalan, and A. Gruverman, Appl. Phys. Lett. **80**, 2740 (2002).
[37]M. J. Haun, E. Furman, S. J. Jang, H. A. McKinstry, and L. E. Cross, J. Appl. Phys. **62**, 3331 (1987).
[38]M. J. Haun, E. Furman, S. J. Jang, and L. E. Cross, Ferroelectrics **99**, 63 (1989).
[39]M. A. Caro, S. Zhang, T. Riekkinen, M. Ylilammi, M. A. Moram, O. Lopez-Acevedo, J. Molarius, and T. Laurila, J. Phys.: Condens. Matter **27**, 245901 (2015).
[40]O. Ambacher, B. Christian, N. Feil, D. F. Urban, C. Elsässer, M. Prescher, and L. Kirste, J. Appl. Phys. **130**, 045102 (2021).
[41]F. Tasnádi, B. Alling, C. Höglund, G. Wingqvist, J. Birch, L. Hultman, and I. A. Abrikosov, Phys. Rev. Lett. **104**, 137601 (2010).
[42]M. Akiyama, T. Kamohara, K. Kano, A. Teshigahara, Y. Takeuchi, and N. Kawahara, Adv. Mater. **21**, 593 (2009).
[43]K. J. Choi, M. Biegalski, Y. L. Li, A. Sharan, J. Schubert, R. Uecker, P. Reiche, Y. B. Chen, X. Q. Pan, V. Gopalan, L.-Q. Chen, D. G. Schlom, and C. B. Eom, Science **306**, 1005 (2004).
[44]C. S. Lynch, Acta Mater. **44**, 4137 (1996).
[45]M. J. Haun, Z. Q. Zhuang, E. Furman, S. J. Jang, and L. E. Cross, Ferroelectrics **99**, 45 (1988).
[46]Z. Li, M. Grimsditch, X. Xu, and S. K. Chan, Ferroelectrics **141**, 313 (1993).
[47]J. F. Nye, *Physical Properties of Crystals: Their Representation by Tensors and Matrices* (Clarendon Press, 1985).
[48]E. Österlund, J. Kinnunen, V. Rontu, A. Torkkeli, and M. Paulasto-Kröckel, J. Alloys Compd. **772**, 306 (2019).
[49]M. D. Henry, T. R. Young, E. A. Douglas, and B. A. Griffin, J. Vac. Sci. Technol. B **36**, 03E104 (2018).
[50]K. Yazawa, J. Mangum, P. Gorai, G. L. Brennecka, and A. Zakutayev, J. Mater. Chem. C (to be published).